RSC Medicinal Chemistry

ROYAL SOCIETY OF CHEMISTRY

REVIEW

View Article Online
View Journal

Cite this: DOI: 10.1039/d6md00223d

Recent advances in piperine and its derivatives as potential anticancer agents

Qi-Hua Yu,[a] Zhiyan Liu,[a] Jiazheng Liu[a] and Li-Ping Bai *[abc]

Piperine, a crucial ingredient of the plant *Piper nigrum*, exhibits a broad spectrum of biological activities and has attracted interest as a potential anticancer agent. Owing to its low yield in natural resources, chemists have developed several synthetic methods for piperine. In addition, the low water solubility and poor bioavailability of piperine have significantly limited its therapeutic applications. Structural modification, particularly at its piperidine moiety, enables the introduction of diverse functional groups to afford piperine derivatives with improved anticancer potency and favorable pharmacodynamic profiles. This article reviews the recent advances (from 2012 to 2025) in the structural characterization, chemical synthesis, biosynthesis, anticancer profile, structural modification, and structure–activity relationships of piperine, which may provide a useful direction for the development of more effective piperine-based anticancer candidates or agents.

Received 20th March 2026,
Accepted 20th May 2026

DOI: 10.1039/d6md00223d

rsc.li/medchem

1. Introduction

Cancer is a serious public health problem in the 21st century, accounting for almost one in six deaths (16.8%).[1] There are several approaches for current cancer treatments, such as chemotherapy, surgery, radiotherapy and biotherapy. Chemotherapy, a conventional cancer therapy, still faces enormous challenges owing to its drug resistance, toxicity, and target mutations.[2] The number of patients requiring chemotherapy is expected to increase by 53% annually, from 9.8 million in 2018 to 15.0 million in 2040.[3] Thus, it is urgent to discover novel anticancer drugs with higher efficacy and lower toxicity for meeting the growing demand of chemotherapy drugs. Natural products have long been a valuable resource for drug discovery due to their chemical diversity and abundant biological activity but relatively low toxicity.[4]

Piperine (Fig. 1), a natural alkaloid, was first isolated from *Piper nigrum* by the Danish scientist Hans Christian Orsted in 1819.[5] Piperine is a weak base in nature, which upon alkaline hydrolysis, decomposes to piperidine and piperic acid derivatives.[6] The structure of piperine (Fig. 1) is composed of three parts: (1) an aromatic region (1,3-benzodioxole group), (2) an aliphatic chain region (butadiene chain), and (3) an amide region (a piperidine ring connected with an α,β-unsaturated carbonyl moiety).[7] In addition, piperine contains four *cis-trans* isomeric structures (Fig. 2) named as the *trans–trans* isomer (piperine), *cis–cis* isomer (chavicine), *cis-trans* isomer (isopiperine), and *trans-cis* isomer (isochavicine).[8]

Piperine is distributed in several members of the Piperaceae family, such as *Piper nigrum*,[9] *P. chaba*,[10] *P. longum*,[11] and *P. guineense*,[12] as the main secondary metabolites. Additionally, piperine has attracted considerable attention from pharmaceutical chemists and nutritional experts due to its multiple biological activities, including anti-cancer,[13] anti-oxidant,[14] anti-inflammatory,[15] neuroprotection,[16] hepatoprotection,[17] antidepressant,[18] and anti-diabetes[19] effects. Hence, there is a strong demand for piperine and for its further research and development. Despite the several biological properties of piperine, its low solubility in water and limited bioavailability have constrained its clinical application, as administration of high doses may be required, which can result in toxicity.[20] Moreover, the low concentration of piperine in *Piper nigrum* and its low extraction yield have limited the practical applications and industrial development of piperine.[21] To overcome these limitations, scientists have not only

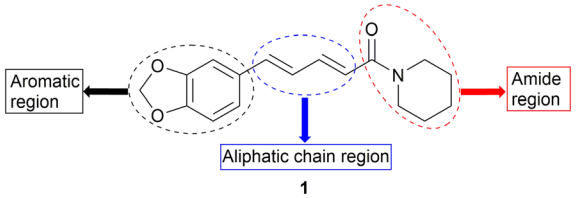

1

Fig. 1 Structure of piperine.

[a] *State Key Laboratory of Mechanism and Quality of Chinese Medicine, Macau Institute for Applied Research in Medicine and Health, Macau University of Science and Technology, Taipa, Macau 999078, China*
[b] *Guangdong-Macao Joint Laboratory for Innovative Drug Research on TCM and Natural-Derived Small RNAs, Macau University of Science and Technology, Taipa, Macau 999078, China*
[c] *Zhuhai M.U.S.T. Science and Technology Research Institute, Hengqin New District, Zhuhai, Guangdong, 519031, China. E-mail: lpbai@must.edu.mo*

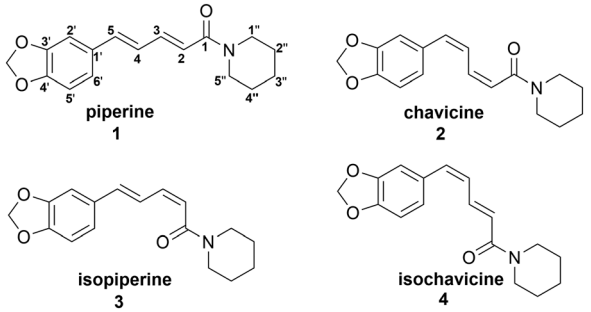

Fig. 2 Isomers of piperine.

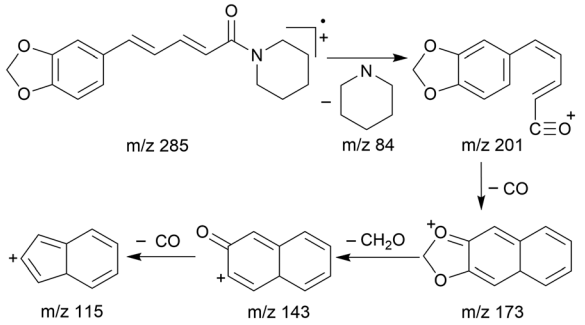

Fig. 3 Mass spectral fragmentation pattern of piperine.

developed several synthetic methods to obtain piperine but also synthesized piperine derivatives to enhance their efficacy.[22]

With the aim to provide deeper insights into the anticancer development of piperine derivatives and expand their therapeutic potential, this review summarizes the recent advances (from 2012 to 2025) in piperine research, including structural characterization, chemical synthesis, biosynthesis, anticancer activity, structural modifications, and structure–activity relationship (SAR) studies.

2. Structural characterization of piperine

Piperine is typically found in the yield range of 1.7–7.4% from the raw black pepper materials.[9] In addition, the main pungency of pepper is caused by piperine. Although the other three isomers are only slightly pungent and are found in very low concentrations in pepper, piperine is gradually converted into chavicine on storage, leading to the loss of pungency.[23] Therefore, several technical methods are needed to determine the chemical structures of piperine and its isomers. In the past few decades, spectroscopic techniques including ultraviolet (UV) spectroscopy, nuclear magnetic resonance (NMR), mass spectrometry (MS), and infrared spectroscopy (IR) have been widely used to elucidate the structural characteristics of piperine.

Due to the geometric isomerism in the two double bonds, piperine **1** (Table 1) was estimated by UV spectroscopy at the UV maximum absorption wavelength of 340 nm and chavicine **2**, isopiperine **3**, and isochavicine **4** at 318, 332, and 333 nm, respectively.[24] Furthermore, as shown in Table 1, the difference between piperine and its isomers in the coupling constants for the olefinic protons (*cis*-$J_{(H,H)} \approx 11$ Hz, *trans*-$J_{(H,H)} \approx 15$ Hz) makes it possible to determine the configuration of the isomers in the ^{1}H spectrum.[24] The mass spectrum of piperine[25] is characterized by the fragment ions (*m*/*z*): 285 molecular ion (M^+), 201 from cleavage at the C–N bond, and 173 representing loss of –CO (28) from *m*/*z* 201, followed by the loss of –CH_2O (30) and –CO (28) to form *m*/*z* 143 and 115, respectively. The genesis of these fragment ions[25–27] can be rationalized, as shown in Fig. 3. In addition, the IR spectrum[24] of piperine exhibits a carbonyl stretching band in the α,β-unsaturated amide moiety, which appears at approximately 1650 cm^{-1}. The alkene C–H, aromatic C–H and aliphatic C–H stretching bands appear at approximately 3080 cm^{-1}, 3030 cm^{-1}, and 2910 cm^{-1}, respectively. The stretching of C═C of aromatic rings was observed in the range of 1606–1483 cm^{-1}, while the stretching of alkene C═C was observed at approximately 1620 cm^{-1}. The asymmetric and symmetric stretching of the methylenedioxy group varies between 1257–1226 and 1143–1128 cm^{-1}, respectively.[26]

Overall, these spectroscopic data (UV, NMR, MS, and IR) collectively support the structural assignment of piperine and facilitate the identification of piperine-type amides in future studies.

Table 1 Comparison of the structural characterization data of piperine and its isomers

Compound	1	2	3	4
UV λ_{max} (nm)	340	318	332	333
NMR $J_{2,3}$ (Hz)	14.7 (*trans*)	11.1 (*cis*)	11.2 (*cis*)	14.7 (*trans*)
NMR $J_{3,4}$ (Hz)	8.5	11.0	11.2	11.8
NMR $J_{4,5}$ (Hz)	15.0 (*trans*)	11.1 (*cis*)	15.6 (*trans*)	11.8 (*cis*)

3. Chemical synthesis of piperine

Although piperine is traditionally extracted from black pepper,[21] the extraction supply may still be constrained by a multistep procedure and variable efficiency. To address these issues, scientists have continued to develop several synthetic strategies for the artificial synthesis of piperine. In this section, we summarize the recent synthetic strategies for piperine.

In 2019, Bauer and co-workers[28] reported the quantitative and stereoselective synthesis of piperine (Scheme 1) by using 2-pyrone (**5**) as the starting compound. The bicyclo[2.2.0] lactone (**6**) was prepared from 2-pyrone (**5**) *via* photochemical synthesis. Subsequently, lactone (**6**) was reacted with copper cyanide (CuCN), lithium chloride (LiCl) and Grignard reagent of the piperonal to obtain the *E*,*E*-diene isomer (**7**) in the copper-mediated nucleophilic addition and electrolytic ring opening reaction. At last, the isomer (**7**) was converted into acyl chloride and then reacted with piperidine to afford piperine (**1**) in more than 95% yield.

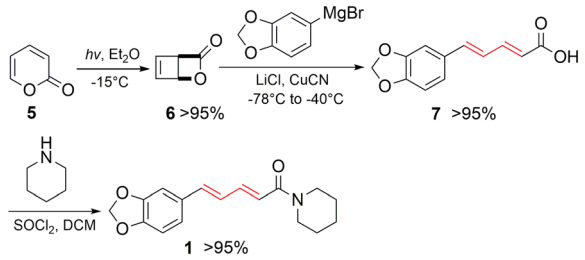

Scheme 1 Bauer *et al.*'s method for the synthesis of piperine.

Tian *et al.*[29] developed an alternative route by using methyl (*E*)-4-bromobut-2-enoate (**8**) and 3,4-dihydroxybenzaldehyde (**9**) as starting materials (Scheme 2) and obtained intermediate **10** and **11**, respectively, *via* nucleophilic substitution reactions. Later, the procedure involved a vinylogous modified Wittig condensation between piperonal (**10**) and the prepared phosphorus ylide reagent (**11**) using LiOH as a base in THF to give methyl piperate (**12**). This transformation is a traditional method to achieve stereoselective control over the double bond configurations.[29–31] Then, piperine (**1**) was prepared by the hydrolysis of **12** and subsequent amidation with piperidine in an overall yield of 65%.

Teskey and co-workers[32] reported a method (Scheme 3) for the selective α,β-dehydrogenation of amides, depending on electrophilic activation coupled to *in situ* selective selenium-mediated dehydrogenation. They published an alternative three-step synthesis starting from the commercially available aldehyde (**11**). After the transformation of **11** into the allylic alcohol (**13**), this compound was treated with the prepared 1,1-diamino alkene (**14**) in refluxing xylene to yield the γ,δ-unsaturated amide (**15**) by a modified Claisen–Eschenmoser rearrangement. Further, compound **15** was reacted with Tf_2O and 2-iodopyridine *via* electrophilic amide activation, and the resulting mixture was subjected to a seleninic acid (PhSe(O)OH)-mediated selective substitution and elimination reaction in the presence of Dess–Martin periodinane (DMP) and Et_3N, affording a late-stage α,β-dehydrogenation tool to access the conjugated amide motif of piperine (**1**) in 42% yield.

In 2022, Keerthana *et al.*[33] described the synthesis of piperine (Scheme 4a) *via* palladium-catalysed aerobic dehydrogenation of γ,δ-olefinic amides. In this method, γ,δ-unsaturated amide (**15**) was dehydrogenated in the presence of

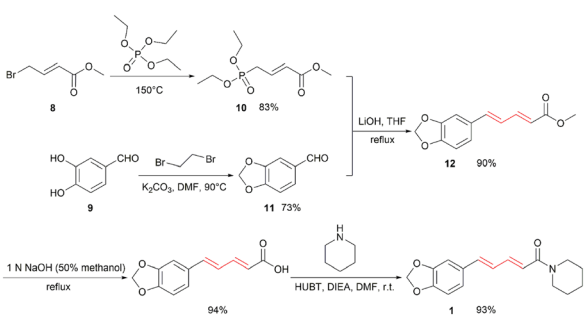

Scheme 2 Tian *et al.*'s method for the synthesis of piperine.

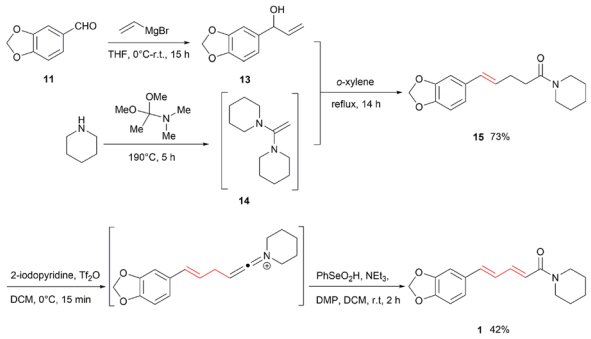

Scheme 3 Teskey *et al.*'s method for the synthesis of piperine.

pivalic acid (PivOH), with $Cu(OAc)_2{\cdot}H_2O$ as a cocatalyst, and 1,2-bis(phenylsulfinyl)ethane as a ligand to obtain piperine (**1**) in 69% yield. In addition, Pan's group[34] developed a new strategy (Scheme 4b) for the direct and efficient synthesis of piperine *via* forming (*E*,*E*)-dienone by a palladium-catalysed aerobic γ,δ-dehydrogenation of enone. Compound **16** was converted into *E*,*E*-dienal (**17**) in the presence of TFA under O_2, followed by oxidation with Jones reagent to an acid and condensation with piperidine to give piperine (**1**) in three steps with an overall yield of 54%.

Li *et al.*[35] reported a β-carbon elimination strategy (Scheme 5) for alkene (sp^2)–C(O) bonds to realize the olefination of unstrained enones *via* vinyl palladium. Their strategy started from the conversion of aldehydes (**11**) to an alkene intermediate (**18**) in the presence of a phosphorus ylide reagent *via* the Wittig reaction. The compound **18** was then reacted with a hydroxylamine reagent to afford a 2,4-di-NO_2-phenyl-substituted oxime ether intermediate, which was subsequently subjected to oxidative addition of palladium, ligand (**19**)-promoted β-carbon elimination, and further cross-coupling with alkene (**20**) to generate the piperine (**1**) *via* a two-step one-pot reaction with 34% overall yield.

Since the earlier report of piperine synthesis by Tsuboi in 1979,[36] improvements and innovations in the geometric control of the diene and in operational simplicity during its synthesis have never stopped. Overall, the recent advances in synthetic chemistry focus on two directions: (1) the efficient construction and stereocontrol of conjugated (*E*,*E*)-diene linkers and (2) the

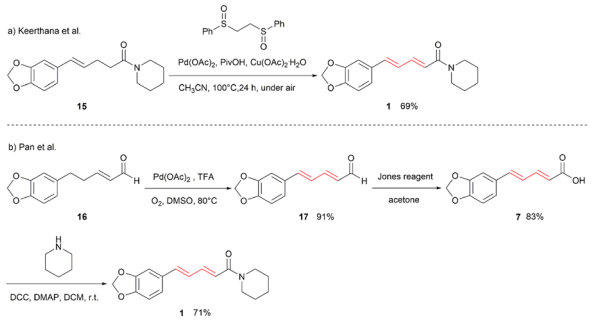

Scheme 4 Palladium-catalysed aerobic dehydrogenation for piperine: (a) Keerthana *et al.*'s method and (b) Pan *et al.*'s method.

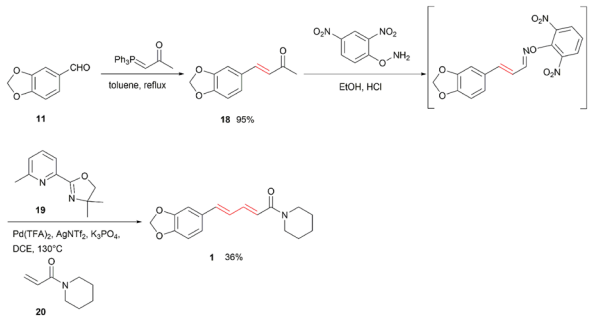

Scheme 5 Li *et al.*'s method for the synthesis of piperine.

development of catalytic dehydrogenation/activation strategies that facilitate the late-stage installation of α,β-unsaturated amides. From the synthesis perspective, piperic acid (or its activated acylating compound) serves as a practical intermediate for coupling with a diverse range of amines. Nevertheless, the main challenges persist in the stereocontrol of *E*/*Z* isomers.

4. Biosynthesis of piperine

Research[37] has shown that the piperine obtained by a complete biosynthetic process mainly consists of two key components: piperidine and piperoyl-coenzyme A. The piperidine heterocycle in piperine is derived from L-lysine, whereas the aromatic part of piperine is derived from L-phenylalanine *via* phenylpropanoid metabolism (Scheme 6).[38] In general, piperine, an alkaloid of secondary metabolites, is biosynthesized through a series of

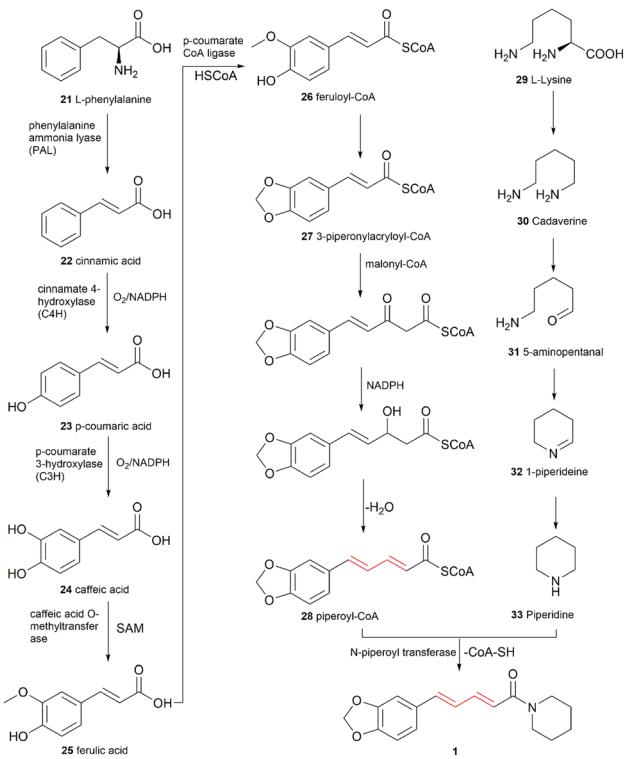

Scheme 6 Hypothetical biosynthesis pathway for piperine.

reactions such as elimination, hydroxylation, condensation, decarboxylation, reduction, oxidative deamination and cyclization.[39,40]

In the biosynthetic pathway of the aromatic part in piperine[38,41] (Scheme 6), L-phenylalanine **21** as a precursor for a broad range of natural products is converted into cinnamic acid **22** by the enzyme phenylalanine ammonia lyase (PAL) *via* the elimination of ammonia. The derivatives of cinnamic acid **22**, such as *p*-coumaric acid **23** and caffeic acid **24**, are formed *via* hydroxylation catalysed by the enzyme in the presence of oxygen and reduced nicotinamide adenine dinucleotide phosphate (NADPH). Additionally, ferulic acid **25** is obtained from caffeic acid **24** *via* an enzyme-catalysed methylation reaction with the co-enzyme *S*-adenosylmethionine (SAM). Thus, it is evident that cinnamic acid and its derivatives are the progenitors for phenylpropanoid compounds. Subsequently, feruloyl-CoA **26** is esterified by ferulic acid **25** and HSCoA with the *p*-coumarate CoA ligase, followed by cyclization to obtain 3-piperonylacryloyl-CoA **27**. As depicted in Scheme 6, several studies[37,38] have proposed that 3-piperonylacryloyl-CoA **27** condenses with malonyl-CoA to form piperoyl-CoA **28**. Similar to the process of fatty acid biosynthesis, the extension on the chain of piperoyl-CoA **28** has been suggested *via* condensation with malonyl-CoA and intermediate **27** through the Claisen reaction, followed by selective reduction and dehydration reaction. However, the malonyl CoA-based chain elongation mechanism proposed for C-2 elongation remains hypothetical and requires direct enzymatic validation.[40,42]

Furthermore, in the biosynthetic pathway (Scheme 6) of the piperidine heterocycle,[25,43] L-lysine **29** is decarboxylated in the presence of the coenzyme pyridoxal phosphate (PLP) to afford cadaverine **30**. Subsequently, cadaverine **30** is subjected to oxidative deamination by the enzyme diamine oxidase to obtain an amino aldehyde **31**. The 5-aminopentanal **31** further undergoes cyclization to yield the imine, 1-piperideine **32**, followed by reduction with NADPH to generate piperidine **33**. Finally, piperine **1** is synthesized in plants from piperidine **33** and piperoyl-CoA **28**. Importantly, an acyltransferase from the shoots of *Piper nigrum* shoots[37] was reported to catalyse piperine formation from piperoyl-CoA and piperidine. This provides a viable biocatalytic strategy for future chemoenzymatic synthesis and late-stage acylation.

5. Anticancer profiles of piperine

Piperine has been reported to exert diverse anticancer effects through multiple mechanisms, including cancer cell cycle arrest and induction of apoptosis and autophagy. Piperine has also been reported to inhibit angiogenesis, invasion, and metastasis through modulating the activities of cancer-relevant enzymes and transcription factors.[2,44] Furthermore, piperine has been investigated as a chemosensitizer to reverse the multidrug resistance (MDR) in cancer cells through its multiple proposed mechanisms (Fig. 4).[45]

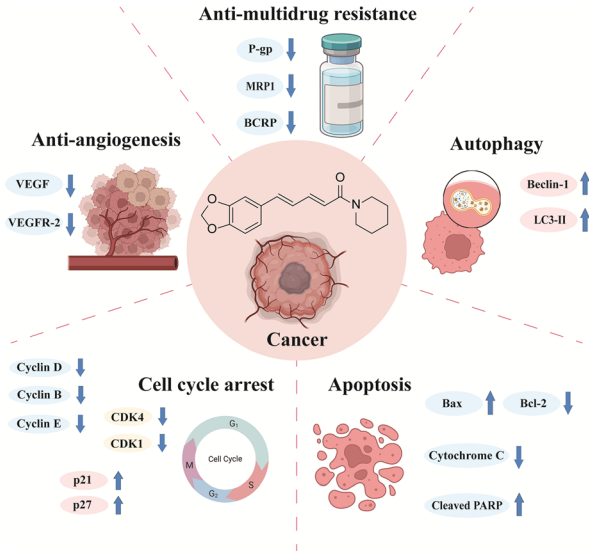

Fig. 4 Anticancer activities of piperine *in vitro*. ↓ denotes the down-regulated protein targets/markers and ↑ denotes the up-regulated protein targets/markers. (The figure was created with https://BioRender.com.).

5.1 Cell cycle arrest, apoptosis, and autophagy

Cancer is associated with irregular, excessive, and continuous proliferation of cells.[46] Several studies have demonstrated piperine-induced cell cycle arrest, apoptosis and autophagy in various cancer cell lines and tumor models. Greenshields *et al.*[47] showed that piperine decreased the expression of cell cycle G1 regulators (cyclin D3, CDK4, and E2F1) and G2 regulators (cyclin B, CDK1, and Cdc25C), as well as increased the expression of $p21^{Waf1/Cip1}$ on the MDA-MB-468 cell line to reduce the percentage of cells in the G2 phase. Chang *et al.*[13] also reported that piperine decreased cyclin E expression and increased p27 levels, consistent with G1 cell cycle arrest in the DLD-1 cell line. In addition, piperine suppressed the phosphoinositide 3-kinase (PI3K)/Akt signaling while increasing the p-extracellular signal-regulated kinase (ERK) levels, which was associated with enhanced apoptotic responses in DLD-1 cells. Besides, Greenshields' group[47] reported that piperine promoted the release of cytochrome c (cyt-c) and second mitochondria-derived activator of caspases/direct inhibitor of apoptosis (IAP)-binding protein with low propidium iodide (PI) (Smac/DIABLO) from the mitochondria to induce caspase-dependent apoptosis in the MDA-MB-468 cell line, without the functional p53. *In vivo*, intratumoral administration of piperine (0.2 mg kg^{-1}) inhibited the growth of MDA-MB-468 cell xenografts in female NOD/SCID nude mice. Han *et al.*[48] reported that piperine downregulated anti-apoptotic protein (B-cell lymphoma-2 protein (Bcl-2)) and upregulated pro-apoptotic protein (Bcl-2-associated X protein (Bax)) and apoptotic marker (cleaved poly (ADP-ribose) polymerase (cleaved PARP)) expression. Meanwhile, piperine also inhibited the PI3K/Akt/mTOR pathway to induce apoptosis in human oral cancer cells (HSC-3). Furthermore, piperine induced autophagy as indicated by increased Beclin-1 expression and LC3-II accumulation in HSC-3 cells. These effects were further supported by investigation in an HSC-3 xenograft mouse model, where piperine suppressed tumor growth. Xia *et al.*[49] reported that piperine induced autophagy-dependent cell death in colorectal cancer (CRC) cells by increasing ROS production and inhibiting Akt/mTOR signaling. *In vivo*, piperine also suppressed tumor growth in a xenograft model of CT26 cell line at a dosage of 20 mg kg^{-1}.

5.2 Anti-angiogenesis

Angiogenesis is a key hallmark of tumor progression, as it is required to supply sufficient oxygen and nutrients to support cancer cell survival and migration, leading to metastasis.[20] Doucette *et al.*[50] demonstrated that piperine inhibited human umbilical vein endothelial cell (HUVEC) proliferation without obvious cytotoxicity. Besides, piperine suppressed HUVEC migration and tube formation *in vitro* and inhibited collagen-induced angiogenesis *ex vivo* in a rat aorta angiogenesis model. Further, piperine reduced MDA-MB-231-induced angiogenesis in the chicken embryo chorioallantois membrane (CAM) model. Li *et al.*[51] reported that piperine inhibited angiogenesis in EA. hy926 endothelial cells induced by lithocholic acid (LCA)-stimulated HCT-116 cells, which occurred through blocking interleukin-8 (IL-8) expression *via* the Src/epidermal growth factor receptor (EGFR)/ROS-mediated ERK1/2 and Akt signaling pathways. Senrung *et al.*[52] also showed that piperine suppressed glioblastoma multiforme (GBM)-induced angiogenesis in a chick CAM U87 glioblastoma xenograft model, accompanied by downregulated vascular endothelial growth factor A (VEGF-A) and VEGF receptor-2 (VEGFR-2) expression.

5.3 Anti-multidrug resistance

Multidrug resistance (MDR) impairs the anticancer efficacy of chemotherapy by reducing the intracellular accumulation of chemotherapeutic drugs in cancer cells through the overexpression of MDR related proteins.[53,54] Piperine could be used in combination with chemotherapeutic agents to reverse MDR, thereby enhancing the anticancer efficacy. Li *et al.*[45] reported that piperine inhibited P-glycoprotein (P-gp), multidrug resistance-associated protein 1 (MRP1) and breast cancer resistance protein (BCRP) expression, which was associated with resensitization to doxorubicin (DOX) and mitoxantrone in resistant cell models, including MCF-7/DOX and A549/cisplatin, respectively. Xu *et al.*[55] also reported piperine inhibited MDR1 expression to decrease P-gp protein in 4T1 cells while enhancing the intracellular accumulation of paclitaxel (PTX), thereby increasing the cell sensitivity to PTX.

5.4 Targets of piperine

The anticancer profiles summarized above indicate that piperine affects several cancer-relevant processes, including cell-cycle progression, apoptosis, autophagy, angiogenesis, and multidrug resistance. However, most reported anticancer effects of piperine are associated with multi-pathway modulation,

whereas direct molecular target validation and structural information on piperine–target interactions remain limited.

Dihydroorotate dehydrogenase (DHODH) represents one of the few molecular targets of piperine with direct structural validation. Several studies showed that DHODH has emerged as a cancer-relevant metabolic target due to its essential roles in mitochondrial redox regulation and ferroptosis.[56,57] Zhang *et al.*[58] reported that piperine exhibited inhibitory activities against *h*DHODH (IC_{50} = 1.73 μM) as an *h*DHODH inhibitor with anticancer effects. Liu *et al.*[59] also identified piperine as a potent inhibitor of *h*DHODH with an IC_{50} value of 0.88 μM. Further enzymatic kinetic analysis showed that piperine exhibited high inhibitory affinity for *h*DHODH, with an inhibitory constant (K_I) of 0.71 μM and a long residence time (RT) of 182.95 min. Direct binding of piperine to *h*DHODH was further supported by CD spectroscopy, intrinsic fluorescence quenching, and isothermal titration calorimetry (ITC), with a dissociation constant (K_D) of 1.97 ± 0.20 μM. The crystal structure of the *h*DHODH-piperine complex showed that the 1,3-benzodioxole ring is positioned in the hydrophobic region of the channel, whereas the carbonyl oxygen forms a hydrogen bond with Tyr356. Therefore, this study provides valuable structural information for piperine-target binding. In addition, MDR-associated ABC transporters, especially P-gp, were regarded as functional targets involved in the chemosensitizing effect of piperine.[45]

Collectively, piperine has impacts on multiple cancer-relevant processes, including cell-cycle arrest, apoptosis, autophagy, angiogenesis, and drug-resistance pathways. However, most proposed anticancer mechanisms are currently supported by pathway-level observations or biomarker evidence rather than definitive target engagement. In this context, the introduction of target-relevant pharmacophores into piperine derivatives has been used as a strategy to enhance biological potency and achieve more clearly defined target-associated activity.

6. Structural modification and improved anticancer activities

Despite its promising anticancer potential, the clinical application of piperine is hindered by limitations such as poor aqueous solubility, low bioavailability, and potential toxicity at high-dose exposure. Accordingly, medicinal chemistry studies have focused on the structural modification of piperine to optimize its physicochemical and pharmacological properties, improve target engagement, and translate these improvements into enhanced anticancer activity. In most reported derivatives, structural modification has mainly been performed at the amide terminus and its adjacent linker, whereas the 1,3-benzodioxole moiety is retained as an important aromatic moiety. Overall, piperine derivatization can be grouped into three main strategies: polarity/ionizability-related modifications, target-oriented terminal pharmacophore modifications, and linker length/unsaturation/scaffold-rigidity modulation. This section summarizes the representative piperine derivatives within these categories, emphasizing changes in biological potency and mechanism-associated phenotypic profiles.

6.1 Polarity/ionizability-related modifications

To address the physicochemical limitation of piperine, several studies have introduced polar or ionizable moieties into the piperine scaffold. In this part, amino acid residues, peptide-like fragments, cyclic dipeptides, and salt-forming groups have been explored to modulate polarity or hydrophilicity with improved cytotoxicity or additional mechanism-related anticancer phenotypes.

Umadevi *et al.*[60] synthesized piperine amino acid derivatives **34–36** (Fig. 5) *via* hydrolysis, acylation, and condensation with amine, and then these derivatives were evaluated for their cytotoxic activity in two human cancer cell lines (MCF-7 and HeLa). All compounds demonstrated over 50% inhibition against MCF-7 and HeLa cell lines at approximately 1 μM. Among them, compound **34**, a histidine-derived analogue bearing an imidazole side chain, exhibited the highest activity against the MCF-7 cell line with an IC_{50} value of 0.74 μM. Similarly, compound **36**, a tryptophan-derived analogue featuring an indole moiety, showed the highest growth inhibition against HeLa cell lines (IC_{50} = 0.74 μM). These results suggest that amino acid conjugation may improve polarity-related properties and contribute to enhanced cytotoxicity for this series.

Based on the polarity-oriented strategy, Rao *et al.*[61] further synthesized a series of piperine-amino acid ester conjugates by replacing the parent amide linkage with a peptide-like bond (–CO–NH–). They evaluated the *in vitro* anticancer activity by an MTT assay with various cancer cell lines (MCF-7, PC-3, and DU-145) (Fig. 5). The amino acid ester derivatives, including L-valine (**37**, with IC_{50} values of 51.00, 49.00, and 44.00 μM against MCF-7, PC-3, and DU-145 cell lines, respectively), exhibited better cytotoxic activity than the parent compound piperine with IC_{50} value > 50.00 μM in the same cell lines. In addition, the conjugation of L-amino acids to piperine may generally enhance the anticancer activity compared to that of their D-amino acid counterparts (*e.g.*,

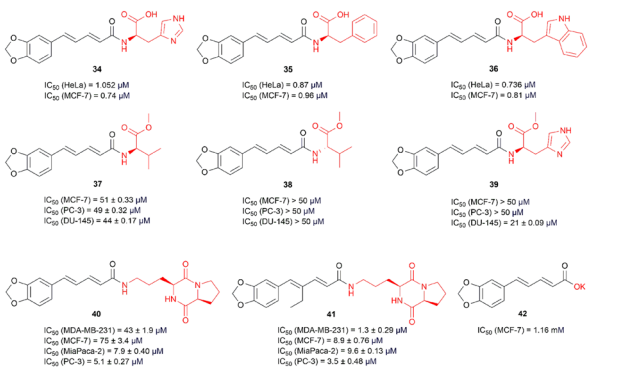

Fig. 5 Chemical structures and anticancer activities of piperine derivatives **34–42**.

L-valine analogue **37** *vs.* D-valine analogue **38**). Notably, the heterocyclic side chain-bearing derivative, such as L-histidine derived analogue **39**, was among the most active, with an IC_{50} value of 21.00 μM in DU-145 cells. These findings indicated that amino acid ester conjugation, particularly with heteroaromatic side chain, can enhance the cytotoxicity of piperine derivatives.

A related peptide-based approach was reported by Shankar *et al.*,[62] who generated four novel piperine derivatives by coupling cyclic dipeptides with piperic acid or 4-ethylpiperic acid scaffolds. Compound **40**, piperic acid-cyclic dipeptides c(Orn-Pro), exhibited better cytotoxicity with an IC_{50} value of 7.90 μM against the MiaPaca-2 cell line. Importantly, compound **41**, 4-ethylpiperic acid-c(Orn-Pro), showed potential cytotoxic activity with IC_{50} = 1.30 μM in MDA-MB-231, 3.50 μM in PC-3, 8.90 μM in MCF-7, and 9.60 μM in MiaPaCa-2 cell lines. Moreover, compound **41** increased E-cadherin while decreasing key mesenchymal markers (Snail, Twist-1, and Vimentin) and metastasis-related proteins (MMP2 and MMP9) to attenuate MDM2-dependent cancer cell metastasis in a p53-independent manner. In the 4T1 mouse xenograft tumor model, compound **41** significantly reduced both the primary tumor weight by 52% and the tumor volume by 65%, while also inhibiting lung metastasis of cancer cells at a safe and tolerable dosage of 20 mg kg^{-1}. Thus, cyclic dipeptide incorporation may not only improve cytotoxic potency but also contribute to anti-metastatic phenotypes.

In addition to amino acid and cyclic dipeptide conjugation, salt formation provides another way to introduce ionizability into piperine-related derivatives. Fan *et al.*[63] demonstrated that the potassium piperonate (GBK) **42** (Fig. 5), an ionized salt form derived from piperic acid, showed cytotoxic activity against MCF-7 cells with an IC_{50} value of 1.16 mM. Further mechanistic studies showed that GBK inhibited the proliferation of breast cancer cells by arresting the G1/S phase transition *via* the upregulation of p27 expression and the inhibition of cyclin A, cyclin E, and cyclin B expression. In addition, GBK induced apoptosis *via* the activation of caspase 6 and caspase 9, and the engagement of the p38/JNK MAPK signaling pathways in MCF-7 cells. *In vitro*, the combination of GBK with etoposide phosphate (VP-16) or cisplatin at Sub-IC_{50} concentrations exerted a synergistic inhibitory effect on the viability of MCF-7 cells. In NOD/SCID mice bearing MCF-7 xenografts, intraperitoneal administration of GBK at 10 mg kg^{-1} showed significant antitumor efficacy, without any obvious change in body weight. Moreover, their group[64] further elucidated that **42** downregulated miR-31-associated pro-metastatic genes, such as *SATB2*, *RHOA*, and *WAVE3*, which was consistent with reduced migration and invasion in SUM-159 and MCF-7 cell lines. In addition, the combination of GBK and cisplatin displayed synergistic anticancer activities against SUM-159 cells in the xenograft model.

Overall, amino acid conjugation, cyclic dipeptide incorporation, and potassium salt formation demonstrate that polarity/ionizability-oriented modification is a useful strategy to improve the anticancer potential of piperine derivatives while retaining the benzodioxole-containing parent scaffold.

6.2 Target-oriented terminal pharmacophore modifications

Compared with polarity-oriented strategies, the modification of the amide terminus with target-relevant pharmacophores can introduce target-recognition or mechanism-associated structural fragments into the piperine scaffold, thereby enhancing enzyme inhibition, kinase inhibition, MDR reversal, anti-angiogenic activity, or cytotoxic potency.

As a terminal modification strategy, Wang's group[65] replaced the piperidine moiety of piperine with aryl-piperazine fragments to generate a series of aryl-piperazine-containing piperine derivatives **43–45** (Fig. 6) and further evaluated their anticancer activity in HeLa and MDA-MB-231 cancer cell lines, as well as human embryonic kidney (HEK) 293 T normal cells, by an MTT assay. As shown in Fig. 6, compound **43**, which retained the piperine scaffold but replaced piperidine with 2-methoxyphenylpiperazine, demonstrated good cytotoxicity against HeLa cells, surpassing that of both 5-fluorouracil (5-FU) (IC_{50} = 44.58 μM) and piperine (IC_{50} = 44.37 μM), while exhibiting relatively low cytotoxicity to HEK293T normal cells. In addition, Zhang's group[66] prepared compound **43** by coupling piperic acid with 1-(2-methoxyphenyl) piperazine and tested its anticancer effects. Compound **43** suppressed colony formation and DNA synthesis in HCT-116 and SW-480 cells. In the CAM xenograft model, it also inhibited HCT116 and SW480 tumor growth and angiogenesis in a dose-dependent manner. Mechanistically, compound **43** impeded

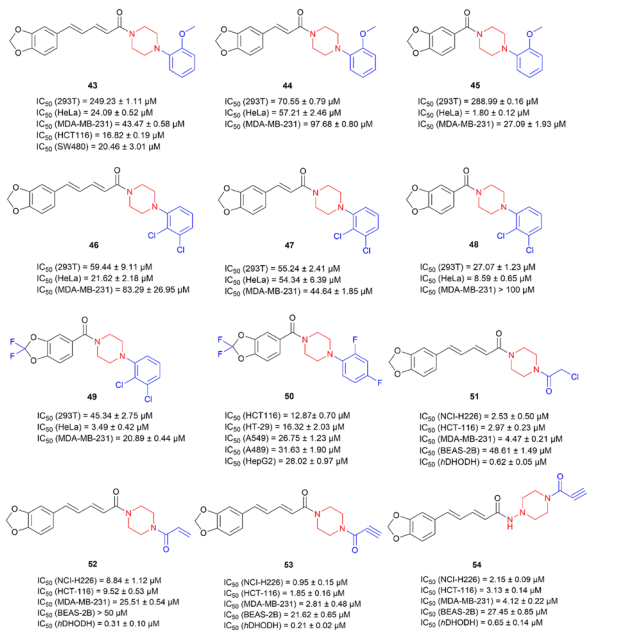

Fig. 6 Chemical structures and anticancer activities of piperine derivatives **43–54**.

tumor progression *via* activating the p53-dependent apoptosis pathway, while it suppressed the Wnt/β-catenin signaling pathway to downregulate the expression of β-catenin and cyclin D1, thereby inhibiting cell proliferation. These findings suggest that the replacement of the piperidine terminus with an aryl-piperazine moiety is an effective terminal modification strategy for enhancing the anticancer profiles of piperine derivatives. Analogues from the same aryl-piperazine series that further involve the linker length or unsaturation modulation, such as **44–50**, are discussed separately in section 6.3.

Zhang *et al.*[58] further designed and synthesized piperazine-containing piperine analogues **51–54** (Fig. 6), and subsequent pharmacological assays revealed that these compounds exhibited low IC_{50} values against cancer cell lines. Both chloroacetamide **51** and propargylamide **53** were more potent in NCI-H226, HCT-116, and MDA-MB-231 cell lines with the IC_{50} values of 2.53 μM, 2.97 μM, and 4.77 μM for **51** and 0.95 μM, 1.85 μM, and 2.81 μM for **53**, than piperine (IC_{50} > 50 μM). SAR studies indicated that introducing an electrophilic ethynyl group (–C≡CH) on a piperazine-linked scaffold was advantageous for improving cytotoxicity. Notably, compound **53** was the most potent human dihydroorotate dehydrogenase (*h*DHODH) inhibitor with an IC_{50} value of 0.21 μM, approximately ten-fold more potent than piperine (IC_{50} = 1.73 μM). In addition, the calculated aqueous solubility (clog *S* = −3.5) and calculated logarithm of the octanol–water partition coefficient (clog *P* = 1.6) of **53** were improved compared with those of piperine (clog *S* = −3.9 and clog *P* = 3.3). Further, compound **53** inhibited NCI-H226 cell proliferation by inducing ferroptosis, as indicated by the changes in lipid peroxidation level, Fe^{2+}, glutathione, and 4-HNE. Molecular docking studies suggested that the carbonyl group adjacent to the ethynyl group formed two direct hydrogen bonds with Arg 136 and Gln 47, while another carbonyl group interacted with Tyr 356, indicating the stabilization of the binding of compound **53** to *h*DHODH.

Besides the piperazine-based terminal modification, aryl-heterocyclic moieties have been incorporated into the piperine scaffold. Amperayani *et al.*[67] designed and synthesized new piperine-oxadiazole and thiadiazole analogs **55–57** (Fig. 7) by coupling amino-substituted oxadiazoles/thiadiazoles with piperic acid through an amide linkage. Among these derivatives, the piperine derivative **55** bearing an oxadiazole moiety with a *para*-hydroxyl group exhibited the highest antiproliferative activity against MCF-7 cells, with a 50% growth inhibition (GI_{50}) value of 2.00 μg mL^{-1}, which was more potent than piperine (GI_{50} = 11.72 μg mL^{-1}), suggesting that the electron-donating hydroxyl substituent was beneficial for antiproliferative activity. Docking studies indicated that compound **55** was docked into the 3EU7 protein pocket, where it was surrounded by the residues of Val-200, Tyr-300, Ala-278, and Phe-300, and formed stable hydrogen bonds. They attributed these interactions to the rigid scaffold of **55** with an amide linkage and hydroxyl groups on heterocyclic moiety, with a low binding energy of −15.23 kcal mol^{-1}.

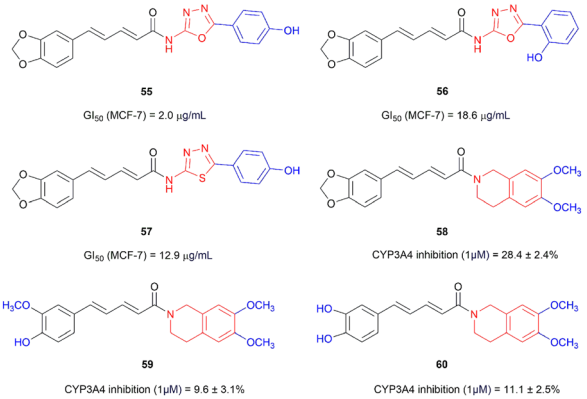

Fig. 7 Chemical structures and anticancer activities of piperine derivatives **55–60**.

Terminal pharmacophore hybridization has also been applied to overcome multidrug resistance. Syed and co-workers[68] synthesized a piperine hybrid as P-gp inhibitors for overcoming multidrug resistance. In an earlier study, piperic acid with a 6,7-dimethoxytetrahydroisoquinoline hybrid **58** (Fig. 7), incorporating a moiety derived from the P-glycoprotein inhibitor elacridar, reversed drug resistance to the chemotherapeutic agents (vincristine, colchicine, and paclitaxel) in P-gp-overexpressing KB and SW480 cancer-resistant cells and outperformed the parent piperine. Further studies demonstrated that compound **58** enhanced the intracellular concentration of these chemotherapeutic drugs in resistant cells by inhibiting P-gp-mediated efflux. Additionally, methoxy substitution was identified as a key group of P-gp inhibitory activity.[68] Syed's group[69] subsequently designed analogues **59–60** (Fig. 7) based on compound **58** *via* the ring-opening of dioxole moiety and methylation. Compound **59** reversed vincristine resistance in KB Ch^R 8–5 cells and was identified as a promising P-gp inhibitor with low CYP3A4 inhibitory activity. It also potentiated the vincristine-induced apoptosis which is medicated by the NF-κB pathway.

In addition to heterocyclic groups, terminal aromatic structural modifications are associated with redox regulation and epigenetic enzyme inhibition. Zhong *et al.*[70] reported two series of piperine-benzene derivatives and tested their cytotoxicity against four cancer cell lines, HeLa, HepG2, SMMC-7721, and A549. As shown in Fig. 8, compound **61**, which was derived from the incorporation of a *meta*-chlorophenyl moiety into the piperine, showed good inhibitory activity with IC_{50} values in the range of 23–38 μM. Its cytotoxic activity (IC_{50} = 23.10 μM) in the HeLa cell line was three-fold more than that of the parent compound piperine (IC_{50} = 85.10 μM). These studies suggested that the *meta*-position electron-withdrawing substitution on the appended phenyl ring potentiated cytotoxicity, whereas the modulation of the conjugated chain length had no discernible effect within this series. Further investigation revealed that compound **61** selectively inhibited TrxR activity *via* binding with the Sec residue, disrupted the redox balance by the generation of additional ROS levels in the cells, and eventually caused apoptosis of HeLa cells.

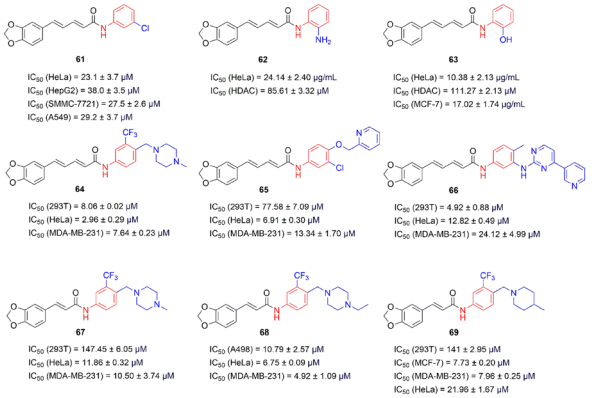

Fig. 8 Chemical structures and anticancer activities of piperine derivatives **61**–**69**.

Somsakeesit *et al.*[71] reported the synthesis of piperine derivatives (Fig. 8) *via* hydrolysis and amidation reactions by coupling piperic acid to 2-aminophenyl (**62**) or 2-hydroxyphenyl (**63**), respectively. Subsequently, the derivatives were evaluated for histone deacetylase (HDAC) inhibition and for cytotoxic activity against the HeLa cell line by an MTT assay. Compound **62** and **63** inhibited HDAC with IC_{50} values of 85.61 μM and 111.27 μM, respectively, outperforming piperine (IC_{50} = 352.80 μM). In addition, compound **63** showed potent cytotoxic activity against HeLa cells with an IC_{50} value of 10.38 μg mL^{-1}. Further docking studies suggested that compound **62**/**63** could form a hydrogen bond toward HDAC active sites and chelate with the Zn^{2+} binding site. The hydroxyl and amino groups were proposed to enhance hydrogen bond formation, whereas the phenyl ring may contribute to hydrophobic interactions and π–π stacking interactions. In addition, their group[72] further reported the anticancer activity of **63** against MCF-7 cells by cytotoxic assays with an IC_{50} value of 17.02 μg mL^{-1}. Further studies demonstrated that compound **63** increased the level of intracellular reactive oxygen species (ROS) and induced apoptosis involving the modulation of DNA repair, estrogen receptor-α (ER-α), and PI3K/Akt pathways.

As shown in Fig. 8, Wang *et al.*[73] synthesized piperine derivatives **64**–**67** by modifying the piperidine part and using a fragment-splicing strategy, in which kinase inhibitory fragments (structural motifs derived from imatinib, neratinib, and ponatinib) were conjugated to the piperine scaffold *via* acyl chloride-mediated amidation. The cytotoxic effect of the modified compounds against HeLa cells was higher than that of the parent compound of piperine (IC_{50} = 44.37 μM) and the positive control drug 5-FU (IC_{50} = 44.58 μM), and their IC_{50} values were mainly in the range of 3–13 μM. Though compound **64** showed the best cytotoxic effect against HeLa and MDA-MB-231 cell lines, it exhibited a lower IC_{50} value (8.06 μM) against the HEK293T cell line, indicating its toxicity towards normal cells. These findings suggest that the replacement of the piperidine terminus with the kinase inhibitory fragment is also a useful strategy for enhancing the anticancer profiles of piperine derivatives. Related analogues in this series that additionally modulate the linker length or unsaturation, such as **67**–**69**, are discussed separately in section 6.3.

Fig. 9 Chemical structures and anticancer activities of piperine derivatives **70**–**72**.

Terminal urea and sulfonamide pharmacophores can transform piperine derivatives into target-oriented enzyme or receptor kinase inhibitors. Elimam *et al.*[74] designed and synthesized a series of piperine-urea derivatives as carbonic anhydrase inhibitors (CAIs) by integrating a benzenesulfonamide fragment inspired by SLC-0111 (a selective *h*CA IX inhibitor) onto the piperine skeleton. These compounds were investigated against four human carbonic anhydrase (*h*CA) isoforms to confirm isoform selectivity. Among the tested compounds, the primary sulfonamido zinc-binding group (ZBG) analogues **70** and **71** (Fig. 9) displayed potent inhibitory activity against *h*CA IX (inhibition constants (K_IS) = 38.7 nM and 68.2 nM, respectively) and *h*CA XII (K_IS = 57.5 nM and 45.6 nM, respectively). Extending the urea linker of the *para*-regioisomer **70** by inserting an ethylene spacer (**71**) increased the inhibition of *h*CA I, II and XII, but reduced *h*CA IX potency, indicating that the linker length tunes isoform preference. Furthermore, compound **70** exhibited significant cytotoxic activity against the MCF-7 cancer cell line with an IC_{50} of 2.17 μM, superior to reference drug staurosporine (IC_{50} = 4.10 μM). Moreover, compound **70** increased the Sub-G1 fraction and decreased the G2/M population compared to the untreated control. SAR studies[74] revealed that the incorporation of a primary sulfonamido moiety as a ZBG on the terminal phenyl ring and the introduction of a urea linker appear to enhance *h*CA IX/XII engagement, consistent with the improved activity towards MCF-7 cells.

In a follow-up study, Elimam and co-workers[75] expanded the urea-based piperine derivatives and evaluated these derivatives against three human cancer cell lines by the MTT assay. Compound **72** (Fig. 9), featuring a *para*-chloro-substituted benzene moiety on the urea terminus, emerged as the most potent anticancer analogue against MDA-MB-231 cells with an IC_{50} value of 18.70 μM, improving in piperine (IC_{50} = 47.80 μM) and 5-FU (IC_{50} = 38.50 μM). Moreover, compound **72** induced apoptosis through the G2/M phase cell cycle arrest and halted DNA synthesis *via* reduction in the S-phase cell population. Further studies showed that compound **72** inhibited VEGFR-2 with IC_{50} = 231 nM in the VEGFR-2 enzymatic assay. Molecular docking studies indicated that **72** could dock into the ATP-binding site of VEGFR-2, and the piperine skeleton formed a key H-bond with Cys919, while the urea carbonyl oxygen and the urea linker engaged Glu885 and Asp1046 *via* additional H-bond interactions to achieve good VEGFR-2 inhibition.

The incorporation of hydrazone or acylhydrazone moieties provides an approach to introduce hydrogen-bonding and aromatic pharmacophore features into piperine. Tantawy's group[76] reported the preparation of a series of novel

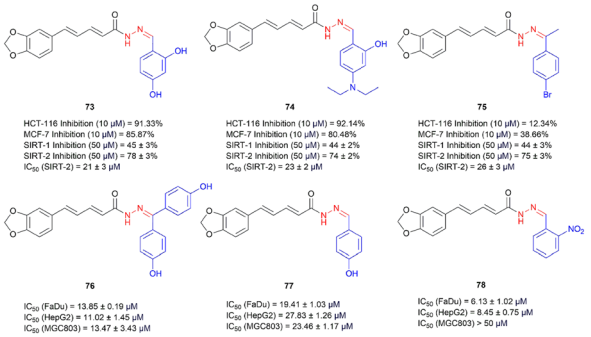

Fig. 10 Chemical structures and anticancer activities of piperine derivatives **73**–**78**.

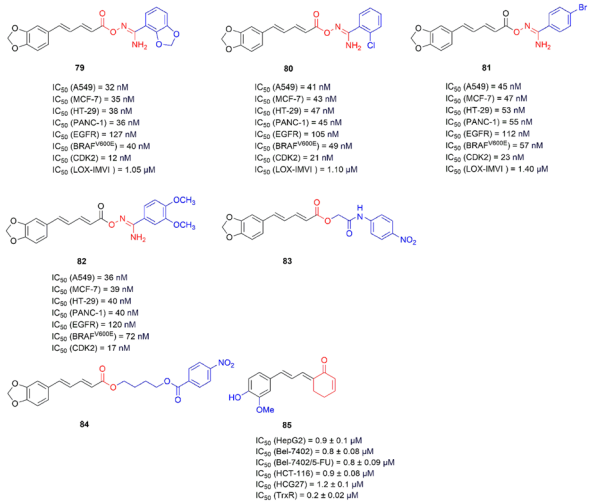

Fig. 11 Chemical structures and anticancer activities of piperine derivatives **79**–**85**.

piperine-hydrazone hybrids with resveratrol-like phenolic pharmacophore moieties *via* hydrolysis, acylation, and conjugation reactions. The cytotoxic activity of the target compounds was examined against sixty cancer cell lines of nine different tissues at a single concentration of 10 μM. The experimental results showed that compound **73**–**75** (Fig. 10) had significant cytotoxic activity. Particularly, compound **73**, possessing a resveratrol pharmacophoric phenolic moiety, showed 91% and 85% growth inhibition in HCT-116 and MCF-7 cells, respectively. Moreover, compounds **73**–**75** exhibited a higher percent inhibition of SIRT2 than SIRT1 at 50 μM. Notably, compound **73** inhibited the SIRT2 enzyme with an IC_{50} value of 21 μM and induced G1-phase cell cycle arrest in MCF-7 cancer cells.

In 2024, Xu *et al.*[77] synthesized a series of novel piperine-hydrazone hybrids **76**–**78** (Fig. 10) and evaluated their anti-proliferative activities in FaDu, HepG2, and MGC803 cells. Compound **76** exhibited significant inhibitory activities against FaDu, HepG2, and MGC803 cells with IC_{50} values of 13.85, 11.02, and 13.47 μM, respectively. In addition, compound **78**, a *meta-nitro*-substituted benzoyl acylhydrazone analogue in this series, exhibited the strongest cytotoxic activity against FaDu and HepG2 with IC_{50} values of 6.13 and 8.45 μM, respectively.

As another example of target-oriented terminal modification, Al-Wahaibi *et al.*[78] developed a series of piperine-carboximidamide hybrids from piperine *via* hydrolysis followed by amidation, and then, evaluated them against several protein kinases and cancer cell lines. Among them, compounds **79**–**82** (Fig. 11) effectively inhibited A549, MCF-7, HT-29, and PANC-1 cell growth, with IC_{50} values ranging from 32 to 55 nM and also showed potent inhibitory effects on EGFR, $BRAF^{V600E}$, and CDK2 kinases with IC_{50} values from 12 to 127 nM. Compounds **79**–**81** also demonstrated promising cytotoxic activity against LOX-IMVI melanoma cells with IC_{50} values ranging from 1.05 to 1.40 μM. Notably, compound **79**, bearing a 1,3-benzodioxole moiety, emerged as the most potent derivative, exhibiting the lowest IC_{50} values. It inhibited MCF-7 cells with an IC_{50} value of 35 nM, outperforming erlotinib (40 nM). Meanwhile, compound **79** also showed the strongest inhibitory activity against CDK2 (IC_{50} = 12 nM), which was 1.7-fold more potent than dinaciclib (IC_{50} = 20 nM). This study indicates that aryl carboximidamide incorporation is a useful strategy for developing piperine-based hybrids with kinase-inhibitory anticancer activity.

Taken together, target-oriented terminal pharmacophore modification provides a viable strategy to convert piperine, an active natural product scaffold, into derivatives with improved target selectivity against *h*DHODH, P-gp, TrxR, HDAC, *h*CA, VEGFR-2, SIRT2, EGFR, $BRAF^{V600E}$, and CDK2.

6.3 Linker length, unsaturation, and scaffold-rigidity modulation

This section focuses on the modulation of linker length, unsaturation degree, and scaffold rigidity. The conjugated diene linker of piperine connects the 1,3-benzodioxole aromatic region to the terminal amide moiety and can affect the electronic distribution and molecular stability.[73,79] Therefore, structural modification of this unsaturated linker can alter cytotoxic potency and anticancer phenotypes.

Within the aryl-piperazine series, modifications to the unsaturated linker affect the anticancer activity. Compared with compound **43**, compound **45** (Fig. 6), which lacks the conjugated unsaturated chain, exhibited the highest potency against HeLa cells (IC_{50} = 1.8 μM) while displaying low cytotoxicity to HEK293T normal cells (IC_{50} = 288.99 μM). Compound **45** also inhibited colony formation, migration, and adhesion of HeLa cells, and suppressed tumor growth and neovascularization in a HeLa xenograft chick embryo model.

Wang's group[80] also synthesized the aryl-piperazine analogues **46**–**49** (Fig. 6) and evaluated their anticancer activity. Compound **49** displayed IC_{50} values of 45.34 μM in the HEK293T normal cell line, 3.49 μM in the HeLa cell line, and 20.89 μM in the MDA-MB-231 cell line, which were better than those of 5-FU and piperine, indicating potent anticancer efficacy with relatively low toxicity. Moreover, compared with compound **46**, compound **49** featured a shortened unsaturated linker and fluorination on the benzodioxole moiety and inhibited

proliferation, adhesion and invasion of HeLa cells *in vitro*. In the chicken embryo model, compound **49** significantly inhibited tube formation and suppressed the growth of HeLa xenograft tumors at a dosage of 10 μg μL^{-1}. SAR analysis[65] suggested that shortening the unsaturated chain and replacing the piperidine with an aryl-piperazine motif improves the *in vitro* potency.

In addition, Zhang's group[81] reported that aryl-piperazine derivative **50** (Fig. 6) showed potent cytotoxic activity against colon cancer cells with IC_{50} values of 12.87 μM (HCT116) and 16.32 μM (HT-29), significantly lower than those of parent piperine (45.62 and 41.32 μM, respectively). Mechanistically, compound **50** downregulated Mki67 expression and activated the p53 pathway, inhibited the E2F pathway, and reduced colorectal cancer cell proliferation, migration, invasion, and angiogenesis in both cell-based and chicken embryo models. These findings suggest that the combination of terminal aryl-piperazine substitution and linker modulation can enhance the anticancer potency.

Within the 1,3-benzodioxole-containing series, the linker length and degree of unsaturation have also been explored. Compared with compound **64**, compound **67** (Fig. 8) featured a shortened conjugated unsaturated linker and showed markedly reduced cytotoxicity toward HEK293T normal cells, with an approximately 18-fold lower IC_{50} value (147.45 μM *vs.* 8.06 μM for **64**), indicating higher selective inhibition (SI) to cancer cells of both HeLa (IC_{50} = 11.86 μM) and MDA-MB-231 (IC_{50} = 10.50 μM). Further biological evaluation exhibited that compound **67** inhibited the proliferation, migration, and adhesion of HeLa cells *in vitro* and significantly suppressed tumor angiogenesis and reduced tumor weight in a chicken embryo model *in vivo*. Moreover, their group[82] designed a series of 1,3-benzodioxole derivatives (a core moiety of piperine essential for antitumor activity) by retaining the 1,3-benzodioxole ring, introducing a vinyl linker and incorporating trifluoromethylpiperazine. Further pharmacological evaluation confirmed that compound **68**, bearing a *para*-ethyl substituent on the aryl-piperazine, showed improved cytotoxic activity against MDA-MB-231 cells (IC_{50} = 4.92 μM) in comparison with 5-FU (IC_{50} = 18.06 μM) and piperine (IC_{50} = 239.03 μM), consistent with *para*-electron-donating substitution as a favorable handle in this series. It also inhibited tumor angiogenesis and reduced the tumor volume and weight without affecting the chick embryo weight in CAM xenograft models. SAR studies[73,82] indicated that this compound, obtained by replacing the piperidine moiety of piperine with an amine side chain containing a trifluoromethyl piperazine moiety and bearing a *para*-substituted electron-donating group on the piperazine ring, may exhibit potent antitumor activity. Additionally, a vinyl linker connecting the benzodioxole core to the amide region appeared to be beneficial for improving the anticancer effect in this series.

Zhou's group[79] also synthesized compound **69** (Fig. 8), an analogue of compound **67**. In particular, compound **69** exhibited lower IC_{50} values of 7.73 μM and 7.96 μM in MCF-7 and MDA-MB-231 cells, respectively, compared with those (13.15 μM and 14.40 μM, respectively) of piperine in the same cell lines. In addition, compound **69** exhibited a reduced cytotoxic effect on HEK293T normal cells (IC_{50} = 141.00 μM) compared to piperine (IC_{50} = 98.11 μM). Compound **69** was found to effectively suppress breast cancer cell proliferation, adhesion, invasion, and migration by inducing cell cycle arrest *via* modulation of the p53/p21-CDK4/6-cyclin D-Rb-E2F pathway. In addition, compound **69** promoted apoptosis in breast cancer cells by modulating the Bax/Bcl-2/Caspase 3 signaling pathway. Docking studies indicated that compound **69** binds within the key hydrophobic pockets of MDM2, yielding an AutoDock Vina score of −10.1 kcal mol^{-1}, which is consistent with a putative inhibition of MDM2-mediated p53 degradation. These studies proposed that the removing the conjugated C═C segment (direct aryl-amide connection) and introducing a trifluoromethyl-substituted aryl unit could modulate the structural and electronic properties and lipophilicity, thereby improving target-relevant interactions and cellular phenotypes.[79,82]

Ester-linked modification represents another strategy to extend the molecular skeleton of piperine analogues. Santos *et al.*[83] prepared piperine-ester analogue **83** (Fig. 11), *N*-(*p*-nitrophenyl)acetamide piperinoate. They tested its toxicity and then evaluated its anticancer effects in the Ehrlich ascites carcinoma (EAC) model. Compound **83** reduced Ehrlich tumor cell viability and peritumoral microvessel density at a dosage of 12.5 mg kg^{-1} *in vivo*. Moreover, compound **83** increased the production of reactive oxygen species (ROS) and nitric oxide (NO). Further, their group[84] synthesized a related analogue **84** (Fig. 11) with an altered linker. Compound **84**, the butyl 4-(4-nitrobenzoate)-piperinoate, showed low acute toxicity, with a lethal concentration 50% (LC_{50}) >100 μg mL^{-1} by the fish embryo toxicity (FET) assay and a lethal dose 50% (LD_{50}) around 1000 mg kg^{-1} (i.p.) in an acute mouse toxicity test. Moreover, compound **84** showed potential antitumor activity in the EAC mouse model at 50 mg kg^{-1}, which was attributed to the modulation of the tumor microenvironment *via* oxidative stress induction and anti-angiogenic effects.

In addition to the ester-linked analogues, Zhu *et al.*[85] designed a series of phenylallylidenecyclohexenone hybrids by integrating the aromatic-olefin-lactam motif of piperlongumine with the α,β-unsaturated carbonyl (enone) moiety of piperine, while replacing the lactam ring with a cyclohexanone. The hybrids were evaluated against five human cancer cell lines and showed IC_{50} values in the range from 0.80 to 8.10 μM, outperforming both the parent piperlongumine and piperine. Among them, compound **85** (Fig. 11) exerted the most potent cytotoxic activity against drug-resistant Bel-7402/5-FU human liver cancer cells with an IC_{50} value of 0.80 μM and low cytotoxicity towards LO2 human normal liver epithelial cells. Meanwhile, the enzymatic activity of TrxR was significantly inhibited by **85**, with an IC_{50} value of 0.20 μM. Mechanistically, compound **85** induced autophagy, accompanied by p38 activation, suppression of the Akt/mTOR signaling pathway, and modulation of LC3, p62 and Beclin-1 proteins.

To sum up, the effects of piperine and its derivatives on the target proteins are presented in Table 2. As shown, piperine derivatives not only displayed strong inhibitory effects on

Table 2 Effects of piperine and its derivatives on the target proteins

Compound	Proteins	IC_{50}	Ref.
1 (piperine)	*h*DHODH	0.88 μM and 1.73 μM	58, 59
53	*h*DHODH	0.21 μM	58
62	HDAC	85.61 μM	71
70	*h*CA IX	38.7 nM	74
71	*h*CA XII	45.6 nM	74
72	VEGFR-2	231 nM	75
73	SIRT-2	21 μM	76
79	EGFR, $BRAF^{V600E}$, and CDK2	127 nM, 40 nM, and 12 nM	78
85	TrxR	0.20 μM	85

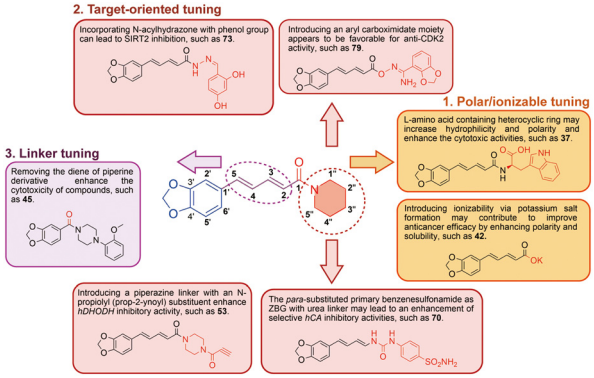

Fig. 12 Graphical depiction of the structure–activity relationships of the piperine derivatives for their anticancer activity.

*h*DHODH, but also showed potential inhibition of other targets, including *h*CA, SIRT-2, and TrXR. Notably, the aryl carboximidamide derivative **79** exhibited excellent inhibitory activity against CDK2, as well as additional target proteins, such as EGFR and $BRAF^{V600E}$.

Based on the cancer-related pharmacological activities of piperine derivatives reported above, the structure–activity relationships (SARs) of piperine derivatives were analyzed and summarized in order to gain insights into the rational optimization of piperine. First, the incorporation of polarity/ionizability-related moieties into piperine, while retaining the 1,3-benzodioxole aromatic moiety, appears to enhance its anticancer efficacy. Notably, the amino acid conjugation serves as an effective method for tuning the polarity of piperine derivatives. The introduction of L-amino acids, especially heteroaromatic amino acids (*e.g.*, histidine **34** or tryptophan **36**), could improve the solubility and modulate the hydrophilicity, thereby contributing to enhanced cytotoxicity. In addition, the conversion to the potassium salt **42** introduces ionizability and increases polarity, which may improve aqueous solubility, thereby contributing to the anticancer efficacy. Second, besides optimizing the physicochemical properties, the piperine scaffold can be modified at the amide terminus with target-relevant pharmacophores to generate piperine hybrids with target selectivity. Mechanistically, terminal pharmacophore cooperation can either strengthen the intrinsic target engagement of piperine or introduce the target-binding moiety, thereby optimizing binding interactions and ultimately enhancing its anticancer activity. Specifically, the terminal introduction of the piperazine linker, followed by the *N*-propargyl (prop-2-ynoyl) group as an electrophilic motif, contributes to enhancing the *hDHODH*-targeted inhibition of piperine (*e.g.*, **53**). The substitution of a *para*-primary benzenesulfonamide Zn^{2+}-binding moiety *via* a urea linker also affords selective inhibition against *h*CA isoforms, while the linker spacer length further modulates isoform selectivity (*e.g.*, **70**/**71**). In addition, the conversion of the terminal amide to an (acyl)hydrazone linkage with phenolic pharmacophore hybridization contributes to SIRT2 inhibition with enhanced cytotoxicity (*e.g.*, **73**). Moreover, the installation of an aryl carboximidamide moiety, in combination with a 1,3-benzodioxole moiety, is favorable for the multi-targeted inhibition activity (EGFR, $BRAF^{V600E}$, and CDK2) with strong cytotoxicity (*e.g.*, **79**). Third, tuning the linker length and unsaturation of the aliphatic chain moiety seems to modulate its cytotoxic potency, with linker shortening being favorable in several series. Notably, in aryl-piperazine-modified piperine derivatives, shortening the linker to a single double bond slightly reduces cytotoxicity, whereas removal of the unsaturated diene chain enhances potency (*e.g.*, **45**). Collectively, these findings demonstrate that both amide terminal modification and aliphatic linker optimization are effective strategies to enhance its anticancer potency while preserving its privileged parent scaffold (Fig. 12).

7. Conclusion and prospects

Piperine, an alkaloid from *Piper nigrum*, is a widely studied natural product scaffold that has shown great potential to motivate extensive structural optimization for anticancer application. This review summarizes the advances (from 2012 to 2025) in the structural characterization, synthesis/biosynthesis, anticancer profile, structural modifications, and structure–activity relationship of piperine-derived anticancer agents. Nevertheless, there are still several limitations, highlighting future directions for developing piperine-based derivatives into viable therapeutic options.

(1) Most anticancer-oriented structural modifications of piperine have focused on the piperidine part, whereas the aliphatic olefin chain remains comparatively underexplored. Future work should be paid more attention to elucidate the SAR and anticancer effects associated with modifications to this aliphatic chain region.

(2) Piperine is a multi-target anticancer compound with activity across diverse cancer types. Accordingly, the hybridization of piperine with other anticancer molecules or suitable pharmacophores may generate hybrids with enhanced efficacy, consistent with the strategy of multi-target drug development.

(3) The piperine derivatives can be predicted and designed by Artificial Intelligence (AI)-assisted approaches, based on molecular targets associated with anticancer activity. AI-

driven structural optimization can accelerate lead compound refinement, potentially enhancing the efficacy while reducing the toxicity.[86] This strategy offers significant promise for the rational design of piperine-based anticancer agents.

(4) Nanoformulation has shown potential to improve drug stability, solubility, and bioavailability.[87,88] In addition, co-administration with bioenhancers exhibits great promise in reducing drug resistance and improving drug efficacy.[89] Exploring innovative approaches for boosting bioavailability properties to enhance the anticancer efficacy of piperine remains a promising direction for future research.

(5) To fully elucidate the anticancer potential of piperine and its derivatives, more *in vivo* investigations are required, as robust *in vitro* potency does not always translate to meaningful efficacy within intact living systems.

It is hoped that this review will be helpful for ongoing research on piperine, and will provide guidance for the advancement of more effective piperine-based anticancer agents.

Conflicts of interest

The authors declare no conflicts of interest for this study.

Abbreviations

SAR	Structure–activity relationship
UV	Ultraviolet spectroscopy
NMR	Nuclear magnetic resonance
MS	Mass spectrometry
IR	Infrared spectroscopy
CuCN	Copper cyanide
LiCl	Lithium chloride
DMP	Dess–Martin periodinane
PivOH	Pivalic acid
PAL	Phenylalanine ammonia lyase
NADPH	Nicotinamide adenine dinucleotide phosphate
SAM	*S*-Adenosylmethionine
CoA	Coenzyme A
PLP	Pyridoxal phosphate
MDR	Multidrug resistance
CDK	Cyclin-dependent kinase
Cdc25C	Cell division cycle 25C
MDA-MB-468	Triple-negative human breast carcinoma cell line
DLD-1	Human colorectal adenocarcinoma cell line
PI3K	Phosphoinositide 3-kinase
Akt	Protein kinase B
ERK	Extracellular signal-regulated kinase
Cyt-c	Cytochrome c
Smac/DIABLO	Second mitochondria-derived activator of caspases/direct IAP-binding protein with low pI
NOD/SCID	Non-obese diabetic/severe combined immunodeficiency
Bcl-2	B-cell lymphoma 2
Bax	Bcl-2-associated X protein
PARP	Poly (ADP-ribose) polymerase
mTOR	Mechanistic target of rapamycin
HSC-3	Human tongue squamous cell carcinoma cell line
LC3-II	Lipidated microtubule-associated protein 1 light chain 3
ROS	Reactive oxygen species
CT26	Murine colon carcinoma cell line
HUVECs	Human umbilical vein endothelial cells
CAM	Chick embryo chorioallantois membrane
LCA	Lithocholic acid
IL-8	Interleukin-8
EGFR	Epidermal growth factor receptor
GBM	Glioblastoma multiforme
VEGF-A	Vascular endothelial growth factor A
VEGFR-2	Vascular endothelial growth factor receptor 2
P-gp	P-glycoprotein
MRP1	Multidrug resistance-associated protein 1
BCRP	Breast cancer resistance protein
DOX	Doxorubicin
PTX	Paclitaxel
HeLa	Human cervical cancer cell line
PC-3	Human prostate cancer cell line
DU-145	Human prostate cancer cell line
IC_{50}	Half-maximal inhibitory concentration
MDA-MB-231	Human triple-negative breast cancer cell line
MCF-7	Human estrogen receptor-positive breast cancer cell line
MiaPaCa-2	Human pancreatic cancer cell line
MMP	Matrix metalloproteinase
MDM2	Mouse double minute 2 homolog
4T1	Murine mammary carcinoma cell line
HEK293T	Human embryonic kidney 293 T cell line
MTT	3-(4,5-Dimethylthiazol-2-yl)-2, 5-diphenyltetrazolium bromide
HCT-116	Human colorectal carcinoma cell line
SW480	Human colorectal adenocarcinoma cell line
5-FU	5-Fluorouracil
HT-29	Human colon adenocarcinoma cell line
NCI-H226	Human lung squamous cell carcinoma cell line
*h*DHODH	Human dihydroorotate dehydrogenase
clog *S*	Calculated logarithm of aqueous solubility
clog *P*	Calculated logarithm of the octanol–water partition coefficient
Arg	Arginine
Gln	Glutamine
Tyr	Tyrosine
GI_{50}	50% growth inhibition concentration
Val	Valine
Ala	Alanine
Phe	Phenylalanine
NF-κB	Nuclear factor kappa-light-chain-enhancer of activated B cells
HepG2	Human hepatocellular carcinoma cell line
SMMC-7721	Human hepatocellular carcinoma cell line
A549	Human lung adenocarcinoma cell line

TrxR	Thioredoxin reductase
Sec	Selenocysteine
HDAC	Histone deacetylase
CAIs	Carbonic anhydrase inhibitors
SLC-0111	A selective human carbonic anhydrase IX inhibitor
ZBG	Zinc-binding group
Cys	Cysteine
Glu	Glutamic acid
Asp	Aspartic acid
SIRT	Sirtuin
FaDu	Human hypopharyngeal squamous cell carcinoma cell line
MGC803	Human gastric carcinoma cell line
PANC-1	Human pancreatic ductal adenocarcinoma cell line
BRAF	B-Raf proto-oncogene, serine/threonine kinase
LOX-IMVI	Human melanoma cell line
JNK	c-Jun N-terminal kinase
MAPK	Mitogen-activated protein kinase
VP-16	Etoposide
SATB2	Special AT-rich sequence-binding protein 2
RHOA	Ras homolog family member A
WAVE3	Wiskott–Aldrich syndrome protein family verprolin-homologous protein 3
SUM-159	Human breast cancer cell line
EAC	Ehrlich ascites carcinoma
NO	Nitric oxide
LC_{50}	Median lethal concentration
LD_{50}	Median lethal dose
FET	Fish embryo toxicity test
i.p.	Intraperitoneal injection
Bel-7402	Human hepatocellular carcinoma cell line
LO2	Human liver cell line
K_I	Inhibitory constant
RT	Residence time
ITC	Isothermal titration calorimetry
K_D	Dissociation constant
SI	Selective inhibition

Data availability

Data sharing does not apply to this article as no datasets were generated or analysed during the current study.

Acknowledgements

This work was financially supported by the Science and Technology Development Fund, Macau SAR (File no. 0137/2022/A3, 0001/2023/AKP, and 0003/2025/NRP). This work was also funded by the Department of Science and Technology of Guangdong Province and supported by the Macao Science and Technology Development Fund (Project No. 2025B1212040001 and 0002/2025/COP).

References

1 F. Bray, M. Laversanne, H. Sung, J. Ferlay, R. L. Siegel, I. Soerjomataram and A. Jemal, *Ca-Cancer J. Clin.*, 2024, **74**, 229–263.
2 M. K. Manickasamy, A. Kumar, B. BharathwajChetty, M. S. Alqahtani, M. Abbas, A. Alqahtani, J. Unnikrishnan, A. Bishayee, G. Sethi and A. B. Kunnumakkara, *Life Sci.*, 2024, **354**, 122943.
3 B. E. Wilson, S. Jacob, M. L. Yap, J. Ferlay, F. Bray and M. B. Barton, *Lancet Oncol.*, 2019, **20**, 769–780.
4 Y. Wang, F. Wang, W. Liu, Y. Geng, Y. Shi, Y. Tian, B. Zhang, Y. Luo and X. Sun, *Pharmacol. Ther.*, 2024, **264**, 108752.
5 J. T. Traxler, *J. Agric. Food Chem.*, 1971, **19**, 1135–1138.
6 A. Tiwari, K. R. Mahadik and S. Y. Gabhe, *Med. Drug Discovery*, 2020, **7**, 100027.
7 H. L. Wiraswati, I. F. Ma'ruf, J. Sharifi-Rad and D. Calina, *BioFactors*, 2025, **51**, e2134.
8 M. Verzele, F. V. Damme and G. Schuddinck, *J. Chromatogr.*, 1989, **471**, 335–346.
9 P. N. Ravindran and J. A. Kallupurackal, in *Handbook of Herbs and Spices*, ed. K. V. Peter, Woodhead Publishing, England, 2nd edn, 2012, ch. 6, vol. 1, pp. 86–115.
10 S. S. Mishra and J. P. Tewari, *J. Pharm. Sci.*, 1964, **53**, 1423–1424.
11 V. C. Verma, E. Lobkovsky, A. C. Gange, S. K. Singh and S. Prakash, *J. Antibiot.*, 2011, **64**, 427–431.
12 H. K. Juliani, A. R. Koroch, L. Giordano, L. Amekuse, S. Koffa, J. A. Dartey and J. E. Simon, in *African Natural Plant Products Volume II: Discoveries and Challenges in Chemistry, Health, and Nutrition*, ed. H. R. Juliani, J. E. Simon and C. T. Ho, American Chemical Society, 2013, ch. 3, vol. 1127, pp. 33–48.
13 W. L. Chang, J. Y. Peng, C. L. Hong, P. C. Li, S. M. Chye, F. J. Lu, H. Y. Lin and C. H. Chen, *Antioxidants*, 2025, **14**, 892.
14 X. Hu, D. Wu, L. Tang, J. Zhang, Z. Zeng, F. Geng and H. Li, *Food Chem.*, 2022, **394**, 133558.
15 Q. N. Baito, H. M. Jaafar and T. A. M. Mohammad, *Cell. Immunol.*, 2023, **391–392**, 104752.
16 R. Nasrnezhad, S. Halalkhor, F. Sadeghi and F. Pourabdolhossein, *Mol. Neurobiol.*, 2021, **58**, 5473–5493.
17 J. Ledesma-Aparicio, P. Mailloux-Salinas, D. J. Arias-Chavez, E. Campos-Perez, S. Calixto-Tlacomulco, A. Cruz-Rangel, J. P. Reyes-Grajeda and G. Bravo, *J. Biochem. Mol. Toxicol.*, 2024, **38**, e70040.
18 Y. S. Wang, C. Y. Shen and J. G. Jiang, *Pharmacol. Res.*, 2019, **150**, 104520.
19 M. Prasad, S. Jayaraman, S. R. Natarajan, V. P. Veeraraghavan, R. Krishnamoorthy, M. K. Gatasheh, C. P. Palanisamy and M. Elrobh, *Int. J. Biol. Macromol.*, 2023, **253**, 127242.
20 E. N. Cinar and N. Sanlier, *Plant Foods Hum. Nutr.*, 2025, **80**, 129.
21 S. Shityakov, E. Bigdelian, A. A. Hussein, M. B. Hussain, Y. C. Tripathi, M. U. Khan and M. A. Shariati, *Eur. J. Med. Chem.*, 2019, **176**, 149–161.

22 W. Cheng, S. Liu, J. He, H. Li, X. Liu, Z. Hu, X. Wang, Z. Wu, G. Xu, W. Liu and B. Liu, *Biochem. Biophys. Res. Commun.*, 2025, **749**, 151323.
23 M. Meghwal and T. K. Goswami, *Phytother. Res.*, 2013, **27**, 1121–1130.
24 W. Ternes and E. L. Krause, *Anal. Bioanal. Chem.*, 2002, **374**, 155–160.
25 É. Szőke, É. Lemberkovics and L. Kursinszki, in *Natural Products*, ed. K. G. Ramawat and J. M. Mérillon, Springer-Verlag, Berlin Heidelberg, Berlin, 2013, ch. 11, pp. 303–341.
26 A. Banerji and P. C. Ghosh, *Tetrahedron*, 1973, **29**, 977–979.
27 M. I. Addae and F. G. Torto, *Tetrahedron Lett.*, 1976, **17**, 3049–3050.
28 A. Bauer, J.-H. Nam and N. Maulide, *Synlett*, 2019, **30**, 413–416.
29 X. Tian, M. Zhou, J. Ning, X. Deng, L. Feng, H. Huang, D. Yao and X. Ma, *J. Enzyme Inhib. Med. Chem.*, 2021, **36**, 737–748.
30 R. A. Olsen and G. O. Spessard, *J. Agric. Food Chem.*, 1981, **29**, 942–944.
31 J. C. Sloop, *J. Chem. Educ.*, 1995, **72**, 25–27.
32 C. J. Teskey, P. Adler, C. R. Goncalves and N. Maulide, *Angew. Chem., Int. Ed.*, 2019, **58**, 447–451.
33 M. S. Keerthana and M. Jeganmohan, *Chem. Commun.*, 2022, **58**, 8814–8817.
34 G. F. Pan, X. L. Zhang, X. Q. Zhu, R. L. Guo and Y. Q. Wang, *iScience*, 2019, **20**, 229–236.
35 H. Li, M.-L. Wang, Y.-W. Liu, L.-J. Li, H. Xu and H.-X. Dai, *ACS Catal.*, 2021, **12**, 82–88.
36 S. Tsuboi and A. Takeda, *Tetrahedron Lett.*, 1979, **20**, 1043–1044.
37 J. G. Geisler and G. G. Gross, *Phytochemistry*, 1990, **29**, 489–492.
38 P. M. Dewick, *Medicinal natural products A biosynthetic approach*, Wiley, United Kingdom, 2009.
39 S. K. Okwute and H. O. Egharevba, *Int. J. Chem.*, 2013, **5**, 99–122.
40 A. Schnabel, F. Cotinguiba, B. Athmer, C. Yang, B. Westermann, A. Schaks, A. Porzel, W. Brandt, F. Schumacher and T. Vogt, *Plant J.*, 2020, **102**, 569–581.
41 Z. Jin, J. Wungsintaweekul, S. H. Kim, J. H. Kim, Y. Shin, D. K. Ro and S. U. Kim, *Biochem. J.*, 2020, **477**, 61–74.
42 Y. Lv, J. Zhu, S. Huang, X. Xing, S. Zhou, H. Yao, Z. Yang, L. Liu, S. Huang, Y. Miao, X. Liu, A. R. Fernie, Y. Ding and J. Luo, *Plant J.*, 2024, **117**, 107–120.
43 G. J. Gatto, N. L. Boyne, N. L. Kelleher and C. T. Walsh, *J. Am. Chem. Soc.*, 2006, **128**, 3838–3847.
44 D. Babadi, S. Dadashzadeh, Z. Shahsavari, S. Shahhosseini, T. L. M. Ten Hagen and A. Haeri, *Int. J. Pharm.*, 2022, **624**, 121990.
45 S. Li, Y. Lei, Y. Jia, N. Li, M. Wink and Y. Ma, *Phytomedicine*, 2011, **19**, 83–87.
46 H. K. Matthews, C. Bertoli and R. A. M. de Bruin, *Nat. Rev. Mol. Cell Biol.*, 2022, **23**, 74–88.
47 A. L. Greenshields, C. D. Doucette, K. M. Sutton, L. Madera, H. Annan, P. B. Yaffe, A. F. Knickle, Z. Dong and D. W. Hoskin, *Cancer Lett.*, 2015, **357**, 129–140.
48 E. J. Han, E. Y. Choi, S. J. Jeon, S. W. Lee, J. M. Moon, S. H. Jung and J. Y. Jung, *Int. J. Mol. Sci.*, 2023, **24**, 13949.
49 J. Xia, P. Guo, J. Yang, T. Zhang, K. Pan and H. Wei, *Biochem. Biophys. Res. Commun.*, 2024, **728**, 150340.
50 C. D. Doucette, A. L. Hilchie, R. Liwski and D. W. Hoskin, *J. Nutr. Biochem.*, 2013, **24**, 231–239.
51 S. Li, T. T. Nguyun, T. T. Ung, D. K. Sah, S. Y. Park, V. K. Lakshmanan and Y. D. Jung, *Antioxidants*, 2022, **11**, 530.
52 A. Senrung, T. Tripathi, J. Yadav, D. Janjua, A. Chaudhary, A. Chhokar, N. Aggarwal, U. Joshi, N. Goswami and A. C. Bharti, *BMC Cancer*, 2023, **23**, 1173.
53 C. R. Quijia and M. Chorilli, *Phytother. Res.*, 2022, **36**, 147–163.
54 A. Manayi, S. M. Nabavi, W. N. Setzer and S. Jafari, *Curr. Med. Chem.*, 2018, **25**, 4918–4928.
55 W. W. Xu, Y. M. Xiao, L. Zheng, M. Y. Xu, X. H. Jiang and L. Wang, *Pharmaceutics*, 2023, **15**, 2703.
56 Z. Zuo, X. Liu, X. Qian, T. Zeng, N. Sang, H. Liu, Y. Zhou, L. Tao, X. Zhou, N. Su, Y. Yu, Q. Chen, Y. Luo and Y. Zhao, *J. Med. Chem.*, 2020, **63**, 7633–7652.
57 C. Mao, X. Liu, Y. Zhang, G. Lei, Y. Yan, H. Lee, P. Koppula, S. Wu, L. Zhuang, B. Fang, M. V. Poyurovsky, K. Olszewski and B. Gan, *Nature*, 2021, **593**, 586–590.
58 J. F. Zhang, L. H. Hong, S. Y. Fan, L. Zhu, Z. P. Yu, C. Chen, L. Y. Kong and J. G. Luo, *Bioorg. Chem.*, 2024, **150**, 107594.
59 Z. Liu, Q. Hu, W. Wang, S. Lu, D. Wu, S. Ze, J. He, Y. Huang, W. Chen, Y. Xu, W. Lu and J. Huang, *Biochem. Pharmacol.*, 2020, **177**, 530.
60 P. Umadevi, K. Deepti and D. V. R. Venugopal, *Med. Chem. Res.*, 2013, **22**, 5466–5471.
61 V. Rama Subba Rao, G. Suresh, R. Ranga Rao, K. Suresh Babu, G. Chashoo, A. K. Saxena and J. Madhusudana Rao, *Med. Chem. Res.*, 2010, **21**, 38–46.
62 S. Shankar, M. M. Faheem, D. Nayak, N. A. Wani, S. Farooq, S. Koul, A. Goswami and R. Rai, *Bioconjugate Chem.*, 2018, **29**, 164–175.
63 L. F. Fan, X. M. Cao, H. J. Yan, Q. Wang, X. X. Tian, L. Zhang, X. Y. He, G. Borjihan and Morigen, *Oncotarget*, 2017, **8**, 47250–47268.
64 X. Tian, J. Lu, K. Nanding, L. Zhang, Y. Liu, M. Mailisu, M. Morigen and L. Fan, *Front. Oncol.*, 2022, **12**, 828160.
65 X.-J. Wang, H.-J. Chen, Z.-Y. Liu, Y. Qiao, X.-B. Wang, B.-Y. Wang, W.-T. Jiang, X. Hou, M.-M. Wang, K.-Q. Li, S.-Y. Zhang, H.-X. Li, B. Liu, J. Ji and M.-L. Yang, *Russ. J. Org. Chem.*, 2024, **60**, 1288–1300.
66 L. Zhang, S. Liu, D. Wang, X. Zhang, Z. Hu, X. Zou, X. Li, X. Wang, D. Xu, W. Liu and B. Liu, *Sci. Rep.*, 2025, **15**, 33541.
67 K. R. Amperayani and U. D. Parimi, *Russ. J. Gen. Chem.*, 2019, **89**, 2301–2307.
68 S. B. Syed, H. Arya, I. H. Fu, T. K. Yeh, L. Periyasamy, H. P. Hsieh and M. S. Coumar, *Sci. Rep.*, 2017, **7**, 7972.
69 S. B. Syed, S. Y. Lin, H. Arya, I. H. Fu, T. K. Yeh, M. R. C. Charles, L. Periyasamy, H. P. Hsieh and M. S. Coumar, *Chem. Biol. Drug Des.*, 2021, **97**, 51–66.
70 M. Zhong, L. Chen, Y. Tao, J. Zhao, B. Chang, F. Zhang, J. Tu, W. Cai and B. Zhang, *Bioorg. Chem.*, 2023, **138**, 106589.

71 L. Somsakeesit, A. Joompang, S. Phosri, P. Srikoon, P. Kumboonma, T. Senawong and C. Phaosiri, *Songklanakarin J. Sci. Technol.*, 2022, **44**, 1481–1488.
72 S. Phosri, A. Naladta, N. Teerakulkittipong, L. O. Somsakeesit, S. Tastub, N. Nualkaew and A. Joompang, *Biochem. Biophys. Res. Commun.*, 2025, **766**, 151895.
73 X. J. Wang, Y. Qiao, X. S. Wang, S. Y. Zhang, H. X. Li, H. H. Hao, K. Q. Li, S. J. Ma, Q. J. Zhu, J. Ji and B. Liu, *Fitoterapia*, 2024, **177**, 106118.
74 D. M. Elimam, A. A. Elgazar, A. Bonardi, M. Abdelfadil, A. Nocentini, R. A. El-Domany, H. A. Abdel-Aziz, F. A. Badria, C. T. Supuran and W. M. Eldehna, *Eur. J. Med. Chem.*, 2021, **225**, 113800.
75 D. M. Elimam, A. A. Elgazar, F. F. El-Senduny, R. A. El-Domany, F. A. Badria and W. M. Eldehna, *J. Enzyme Inhib. Med. Chem.*, 2022, **37**, 39–50.
76 A. H. Tantawy, X. G. Meng, A. A. Marzouk, A. Fouad, A. H. Abdelazeem, B. G. M. Youssif, H. Jiang and M. Q. Wang, *RSC Adv.*, 2021, **11**, 25738–25751.
77 S. K. Xu, Z. M. Jia, W. Q. Liu, Y. Z. Gu, J. H. Xi, J. Xu, G. Z. Yang, X. Z. Yang and Y. Chen, *Nat. Prod. Res.*, 2024, 1–6.
78 L. H. Al-Wahaibi, M. A. Mahmoud, Y. A. Mostafa, A. E. Raslan and B. G. M. Youssif, *J. Enzyme Inhib. Med. Chem.*, 2023, **38**, 376–386.
79 C. Zhou, J. Wang, L. Zhou, H. Li, X. Liu, S. Wang, X. Zhang, X. Ye, H. Ren, K. Zeng, X. Li, D. Wang and J. Ji, *Bioorg. Med. Chem. Lett.*, 2025, **123**, 130231.
80 X. J. Wang, W. N. Jiang, J. J. He, H. J. Chen, Y. Qiao, D. Wang, B. Y. Wang, X. Hou, W. Liu, T. Geng, S. Y. Zhang, X. Liu, S. J. Ma, B. Liu, M. L. Yang and J. Ji, *Chem. Res. Chin. Univ.*, 2024, **45**, 20230520.
81 M. Zhang, R. Liu, W. Jiang, H. Li, S. Zhang, W. Cheng, X. Ye, J. He, Y. Liu, A. Jing, Y. Song, D. Wang, X. Liu, B. Zhang, X. Wang and J. Ji, *Naunyn-Schmiedeberg's Arch. Pharmacol.*, 2025, **398**, 7121–7131.
82 X. J. Wang, B. Y. Wang, B. Zhang, L. Chen, K. Q. Li, M. M. Wang, H. H. Hao, M. X. Lu, X. X. Shen, Y. K. Sun, Z. D. Gao, Z. Y. Yan, Z. Y. Lang, M. J. Yu, Z. J. He, S. J. Ma, J. Ji and Y. L. Chang, *Fitoterapia*, 2025, **187**, 106911.
83 J. Santos, M. Brito, R. Ferreira, A. P. Moura, T. Sousa, T. Batista, V. Mangueira, F. Leite, R. Cruz, G. Vieira, B. Lira, P. Athayde-Filho, H. Souza, N. Costa, R. Veras, J. M. Barbosa-Filho, H. Magalhaes and M. Sobral, *Int. J. Mol. Sci.*, 2018, **19**, 2594.
84 R. C. Ferreira, T. M. Batista, S. S. Duarte, D. K. F. Silva, T. M. H. Lisboa, R. F. P. Cavalcanti, F. C. Leite, V. M. Mangueira, T. K. G. Sousa, R. A. Abrantes, E. O. D. Trindade, P. F. Athayde-Filho, M. C. R. Brandao, K. C. P. Medeiros, D. F. Farias and M. V. Sobral, *Biomed. Pharmacother.*, 2020, **128**, 110247.
85 P. Zhu, J. Qian, Z. Xu, C. Meng, J. Liu, W. Shan, W. Zhu, Y. Wang, Y. Yang, W. Zhang, Y. Zhang and Y. Ling, *J. Nat. Prod.*, 2020, **83**, 3041–3049.
86 K. Zhang, X. Yang, Y. Wang, Y. Yu, N. Huang, G. Li, X. Li, J. C. Wu and S. Yang, *Nat. Med.*, 2025, **31**, 45–59.
87 L. Huang, X. H. Huang, X. Yang, J. Q. Hu, Y. Z. Zhu, P. Y. Yan and Y. Xie, *Pharmacol. Res.*, 2024, **201**, 107100.
88 K. H. Wong, Y. Wang, X. Wang, Y. Yin, K. Feng and M. Chen, *J. Controlled Release*, 2025, **382**, 113656.
89 H. Heidari, M. Bagherniya, M. Majeed, T. Sathyapalan, T. Jamialahmadi and A. Sahebkar, *Phytother. Res.*, 2023, **37**, 1462–1487.

